Supporting Information

Adaptive Mutations Alter Antibody Structure and Dynamics during Affinity Maturation

Ramkrishna Adhikary,[†] Wayne Yu,[†] Masayuki Oda,[¶] Ross C. Walker,[§] Tingjian Chen,[†] Robyn L. Stanfield,[‡] Ian A. Wilson,[‡] Jörg Zimmermann,[†] and Floyd E. Romesberg[†]*

[†]*Department of Chemistry and* [‡]*Department of Integrative Structural and Computational Biology and The Skaggs Institute for Chemical Biology, The Scripps Research Institute, 10550 North Torrey Pines Road, La Jolla, CA 92037, USA.*
[¶]*Graduate School of Life and Environmental Sciences, Kyoto Prefectural University, 1-5, Hangi-cho, Shimogamo, Sakyo-ku, Kyoto 606-8522, Japan.*
[§]*Department of Chemistry and Biochemistry, San Diego Supercomputer Center, University of California San Diego, La Jolla, CA 92093, USA.*

Supplemental Methods

MD simulation for MPTS-6C6 structure

A total of seven simulations were setup and run in an identical fashion. Initial coordinates for Ab 6C6 were generated by side-chain replacement from the crystal structure of Ab 6C8. The AMBER FF99SB force field[1] was used for the amino acids while the AMBER GAFF force field[2] was used for the ligands with AM1BCC[3] charges generated using Antechamber and the SQM package[4] from the AmberTools v13 package.[5,6] The zinc atoms were modeled as ions of charge +2. The system was solvated in an orthorhombic box of TIP3P water molecules [7] such that no solute atom was within 10 Å of any box edge. Finally sufficient Na^+ or Cl^- ions were placed randomly in the solvent box to neutralize the system.

The system was minimized using 5000 steps of steepest descent followed by 5000 steps of conjugate gradient in order to remove steric clashes caused by hydrogenation and solvation. Heating was then conducted in two phases. In the first phase, a simulation of 20 ps was run at constant volume using a Langevin thermostat with a collision frequency of 1.0 ps^{-1}. The target temperature was scaled linearly from 0 to 100 K over the simulation. In the second phase of heating, the simulation mode was switched to isotropic constant pressure, at 1 atm, adding a Berendsen barostat with a relaxation time of 1.0 ps. Heating with a Langevin thermostat was then conducted over 1 ns with the target temperature being linearly scaled from 100 to 310 K. Following the heating, 1 ns of equilibration at constant pressure was performed with a target temperature of 310 K. Production simulations were then run for a further 100 ns using the same protocol as the equilibration. At the end of this, the system was gradually cooled to 0 K over 10 ns of simulation to yield an effective minimized structure.

A time step of 2.0 fs was used for the simulation. Shake was used to constrain all bonds involving hydrogens. A direct-space and vdW cut off of 9.0 Å was used for all simulations and periodic boundaries coupled with the Particle Mesh Ewald (PME) were used to include long-range electrostatic interactions. Structural and energy data was recorded every 2 ps. In all cases, the random seed was based on the wall clock time in microseconds.

All calculations were run with the SPFP precision model[8] using the PMEMD.cuda MD engine[9] (up to and including bugfix.19) from the AMBER 12 software suite[5,6] using NVIDIA GTX680, Titan and K20 GPUs on in house resources. Post simulation analysis was conducted using the cpptraj program [10] from the AmberTools v13 software suite.

3PEPS and transient grating (TG) spectroscopy

The laser source was a Ti:sapphire regenerative amplifier system (Spitfire, Spectra Physics). The

compressed output consists of ~45 fs pulses with energies of 140 – 150 μJ. Approximately 30% of the amplified fundamental beam (836 nm) was frequency-doubled (416 nm, 200 nJ) in a 0.1 mm, Type I LBO crystal. The frequency-doubled pulses were separated with a dichroic mirror from fundamental, and collimated using a pair of lenses. The pulses were further compressed by a pair of fused silica prisms and split into three roughly equal portions with beam splitters. The three beams were arranged in an equilateral triangle (~7 mm per side) and focused on the sample with a plano-convex fused silica lens (200 mm focal length). A spinning cell with a path length of 250 μm was used. Typical pulse energies at the sample were 20 – 25 nJ per pulse. The photon echo signals in the two phase-matched directions k_1-k_2+k_3 and -k_1+k_2+k_3 were spatially filtered and detected with two large area avalanche photodiodes (Advanced Photonics) connected to lock-in amplifiers (Stanford SR830) referenced to a phase-locked chopper (New Focus), and synchronized with the Q-switch of the regenerative amplifier. The delay between the first and second pulses (coherence period, τ) was scanned from -150 to 150 fs for a fixed delay between the second and third pulses (population period, T). T was scanned from 0 to 400 ps with 30 to 40 scans for each T. The peak shift (τ^*) for the two phase-matching directions for a given T were determined by averaging the peak maxima of Gaussian fits of the two temporal signals. At least three independent experiments were carried out for each MPTS-Ab complex from three freshly prepared biological samples. In addition, the terminal peak shift at T = 100 ps of the MPTS/water and MPTS/EtOH were measured each day before collecting data from MPTS-Ab samples to ensure reproducibility. For the TG measurements, τ was set to zero, and T was scanned from 0 to 400 ps. Twenty to 30 scans were averaged for each TG measurement. Transient grating fit parameters are listed below:

	6C6	6C8	8B10
a_1 (%)	29.5 ± 2.6	31.4 ± 1.1	30.9 ± 3.8
τ_1 (fs)	170 ± 13	160 ± 8	170 ± 7
a_2 (%)	29 ± 11	21.4 ± 0.3	21.7 ± 1.8
τ_2 (ps)	1.68 ± 0.46	1.33 ± 0.15	1.36 ± 0.01
a_3 (%)	21.9 ± 3.2	20.2 ± 0.3	21.3 ± 2.2
τ_3 (ps)	15.5 ± 1.0	12.9 ± 1.3	14.6 ± 0.6
a_4 (%)	17.4 ± 2.1	21.4 ± 0.6	19.2 ± 1.9
τ_4 (ps)	115 ± 22	133 ± 6	84 ± 3
a_5(%)	3.7 ± 1.2	5.6 ± 0.3	6.8 ± 0.9

The 3PEPS decays were fit to a sum of exponential decays using Origin 6.0 (Microcal) to evaluate the number of time scales present in the 3PEPS decays. This analysis indicated that at least three exponential decay terms and an offset were required to fit the decays. The 3PEPS decays were then fit using a model spectral density function.[11] In this analysis, both the steady-state absorption spectra and the 3PEPS decay were fit simultaneously by least-squares error analysis, as described below. Briefly, the total spectral density ($\rho(\omega)$) was calculated as the sum of the vibrations of the chromophore ($\rho_{MPTS}(\omega)$) and the vibrations of the protein ($\rho_{Ab}(\omega)$). In a previous study, intramolecular vibrational frequencies and excitation-induced displacements of MPTS were calculated from quantum chemical calculations and also validated experimentally.[12] The $\rho_{Ab}(\omega)$ was modeled as the sum of underdamped ($\rho_{BO}(\omega)$) and overdamped ($\rho_K(\omega)$) Brownian oscillator terms to represent fast (subpicosecond inertial

protein motions) and slower (picosecond protein motions) dynamics respectively. $\rho_{BO}(\omega)$ is given by

$$\rho_{BO}(\omega) = \frac{2\lambda_{BO}}{\pi\omega} \frac{\omega_{BO}^2 \Gamma_{BO}}{(\omega_{BO}^2 + \omega^2)^2 + \Gamma_{BO}^2 \omega^2}$$

where λ_{BO}, ω_{BO} and Γ_{BO}, are the reorganization energy, frequency, and damping constant of the Brownian oscillator, respectively. $\rho_K(\omega)$, also known as the Kubo term, is represented by

$$\rho_K(\omega) = \frac{\lambda_{Ki}}{\pi\omega} \frac{\tau_{Ki}}{(1 + \omega^2 \tau_{Ki}^2)}$$

where λ_K is the reorganization energy and τ_K is the time constant of the Kubo oscillator. Experimental 3PEPS signals and the steady-state absorption spectra were obtained from the line-broadening function $g(t)$ using standard procedures.[11,13,14] The $g(t)$ is expressed by

$$g(t) = i\int_0^\infty d\omega\rho(\omega)\sin(\omega t) + \int_0^\infty d\omega\rho(\omega)\coth\left(\frac{\hbar\omega}{2k_B T}\right)[1 - \cos(\omega t)] + \frac{(\Delta_{inh} t)^2}{2}$$

The best fit for the experimental 3PEPS data and the steady state absorption spectra were obtained by varying the parameters in $\rho_{Ab}(\omega)$ and the amount of static inhomogeneity, Δ_{inh}, in $g(t)$. A least-squares Simplex fit algorithm was used for the best fit of experimental 3PEPS data, however, a custom suite of C programs (Dr. Delmar Larsen, University of California, Davis) was used for the best fit of the steady state absorption spectra. The ω_{BO}, and Γ_{BO} values were fixed to the average values as obtained from fitting 3PEPS decays freely. Spectral densities of all Ab-MPTS complexes are also shown in **Figure S2, panel B**. A representative steady-state absorption spectrum and 3PEPS decay of MPTS-8B10 is shown in **Figure S2, panel C**. The normalized reorganized energies of the Brownian oscillator, Kubo oscillator and the static inhomogeneity ($\lambda_{inh} = \Delta_{inh}^2/2k_B T$, $T = 298$ K) are listed below:

	λ_{BO} (%)	λ_{K1} (%)	λ_{K2} (%)	λ_{inh} (%)[a]
6C6	67.0 ± 4.3	10.4 ± 5.8	15.5 ± 1.1	7.2 ± 1.0
6C8	72.5 ± 5.3	17.6 ± 1.4	9.9 ± 2.4	0.0 ± 0.0
8B10	67.9 ± 3.8	16.1 ± 1.1	16.1 ± 3.0	0.0 ± 0.0

Table S1. Absorption spectral parameters

	λ_{max}(nm)	fwhm (nm)
MPTS/water	403.7	20.0
MPTS/6C6	406.1	17.5
MPTS/6C8	406.2	17.5
MPTS/8B10	406.2	17.6

Table S2. Thermodynamic parameters of the interaction between MPTS and IgG[a]

	T (ºC)	n (M^{-1})	K_a (kcal/mol)	ΔG (kcal/mol·ºC)	ΔH	$T\Delta S$	ΔC_p
6C6							
	20.0	1.71	5.09×10^7	–10.33	–10.29	0.04	–0.125
	25.0	1.68	2.82×10^7	–10.16	–11.05	–0.89	
	25.0	1.75	2.56×10^7	–10.10	–11.02	–0.92	
	30.0	1.60	2.92×10^7	–10.35	–11.60	–1.25	
	35.0	1.68	1.13×10^7	–9.94	–12.20	–2.26	
6C8							
	20.0	1.55	2.04×10^6	–8.46	–8.08	0.38	–0.119
	25.1	1.61	2.34×10^6	–8.69	–8.59	0.10	
	25.1	1.49	3.30×10^6	–8.89	–8.67	0.22	
	25.2	1.42	1.27×10^6	–8.33	–8.55	–0.22	
	30.0	1.40	1.13×10^6	–8.39	–9.25	–0.86	
	34.9	1.55	6.64×10^5	–8.20	–9.67	–1.47	
	35.0	1.43	8.93×10^5	–8.39	–9.94	–1.55	
8B10							
	20.0	1.80	1.65×10^7	–9.68	–10.57	–0.89	–0.116
	25.0	1.73	8.48×10^6	–9.45	–11.11	–1.66	
	25.2	1.76	1.04×10^7	–9.58	–11.13	–1.55	
	30.0	1.81	8.20×10^6	–9.54	–11.74	–2.20	
	35.0	1.79	4.15×10^6	–9.33	-12.28	–2.95	

[a]All measurements were performed for MPTS injection into IgG in PBS (pH 7.4).

Table S3. Proteins used for ELISA[a]

	protein	stock solution
1	Peroxidase	1.0 mg/mL
2	C3G Peptide	2.2 mg/mL
3	Stoffel fragment of Taq DNA polymerase (SF)	n.d.
4	Lysozyme	1.0 mg/mL
5	Human serum albumin	1.0 mg/mL
6	ACTH (1-17)	0.01 mg/mL
7	Rabbit serum albumin	1.0 mg/mL
8	Phosphorylase B	0.05 mg/mL
9	Neurotensin I	0.01 mg/mL
10	Aprotinin	1.0 mg/mL
11	Angiotensin I	0.01 mg/mL
12	ACTH (18-39)	0.01 mg/mL
13	Acylase I	1.0 mg/mL
14	ACTH (7-38)	0.01 mg/mL
15	Taq DNA polymerase	250 units/mL
16	DNAse I	1.0 mg/mL
17	n-SH3 Crk-II	0.9 mg/mL
18	Myoglobin (horse heart)	1.0 mg/mL
19	Lectin	1.0 mg/mL
20	Yeast lytic enzyme	1.0 mg/mL
21	RNAse A	0.5 mg/mL
22	Bovine cytochrome *c*	1.0 mg/mL
23	Triose phosphate isomerase	0.01 mg/mL
24	M13-Phase	n.d.
25	Cyt *c* reductase	n.d.
26	Yeast cyt *c*	1.0 mg/mL
27	RecA	0.1 mg/mL
28	Protein disulfide isomerase	0.5 mg/mL
29	Luteotropic hormone (prolactin)	1.0 mg/mL
30	Cathepsin B	0.5 mg/mL
31	Ubiquitin	0.5 mg/mL
32	Phosphodiesterase	0.1 mg/mL
33	Superoxide dismutase	0.2 mg/mL
34	Fibroblast growth factor	0.01 mg/mL
35	Bovine hemoglobin	1.0 mg/mL
36	T7-Phage	n.d.
37	Porcine hemoglobin	1.0 mg/mL
38	Human hemoglobin	1.0 mg/mL
39	TEV Protease	0.1 mg/mL
40	K50 bicoid homeodomain	1.0 mg/mL
41	Cytochrome P450	1.5 mg/mL
42	MBP-galactosidase	0.04 mg/mL
43	Horse hemoglobin	1.0 mg/mL
44	Concavalin A	1.0 mg/mL
45	spDHFR	4.5 mg/mL

[a]Proteins are arranged according to the increasing binding affinity with 6C8 Ab.

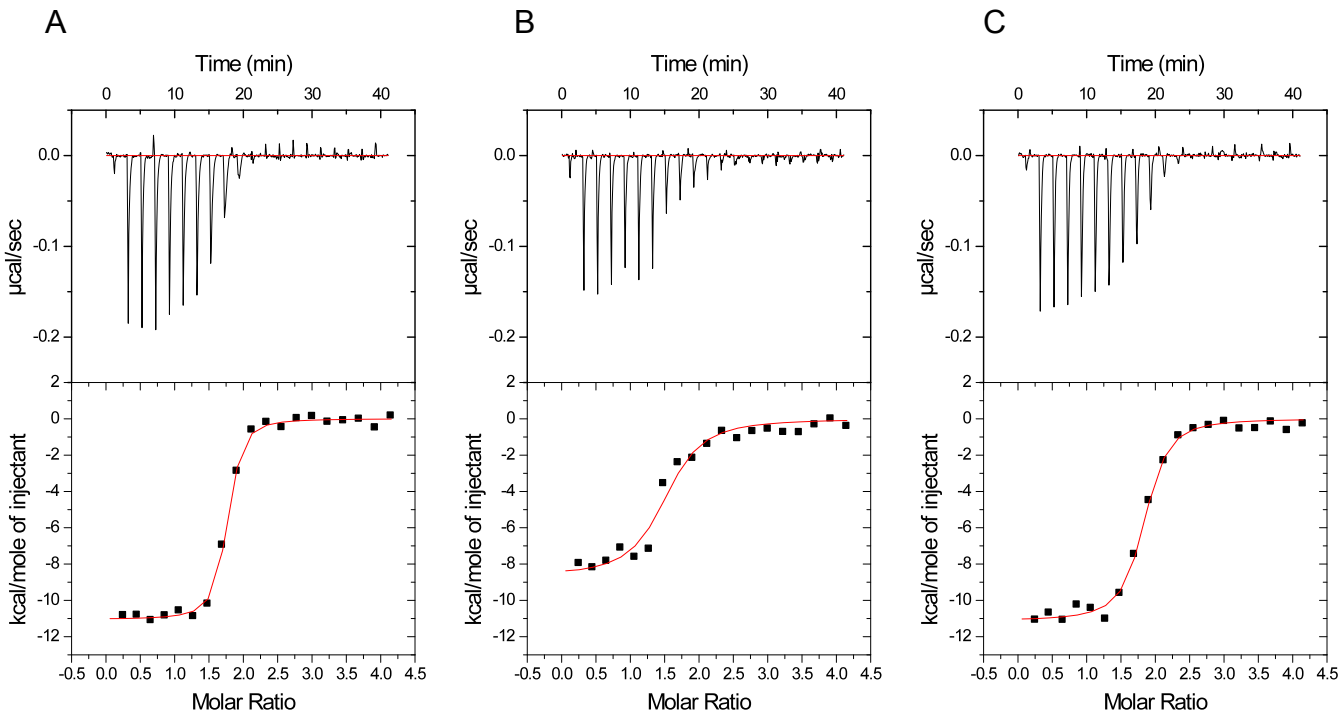

Figure S1. Representative calorimetric titration of IgG. (A) 6C6, (B) 6C8, and (C) 8B10 with MPTS in PBS (pH 7.4) at 25 °C.

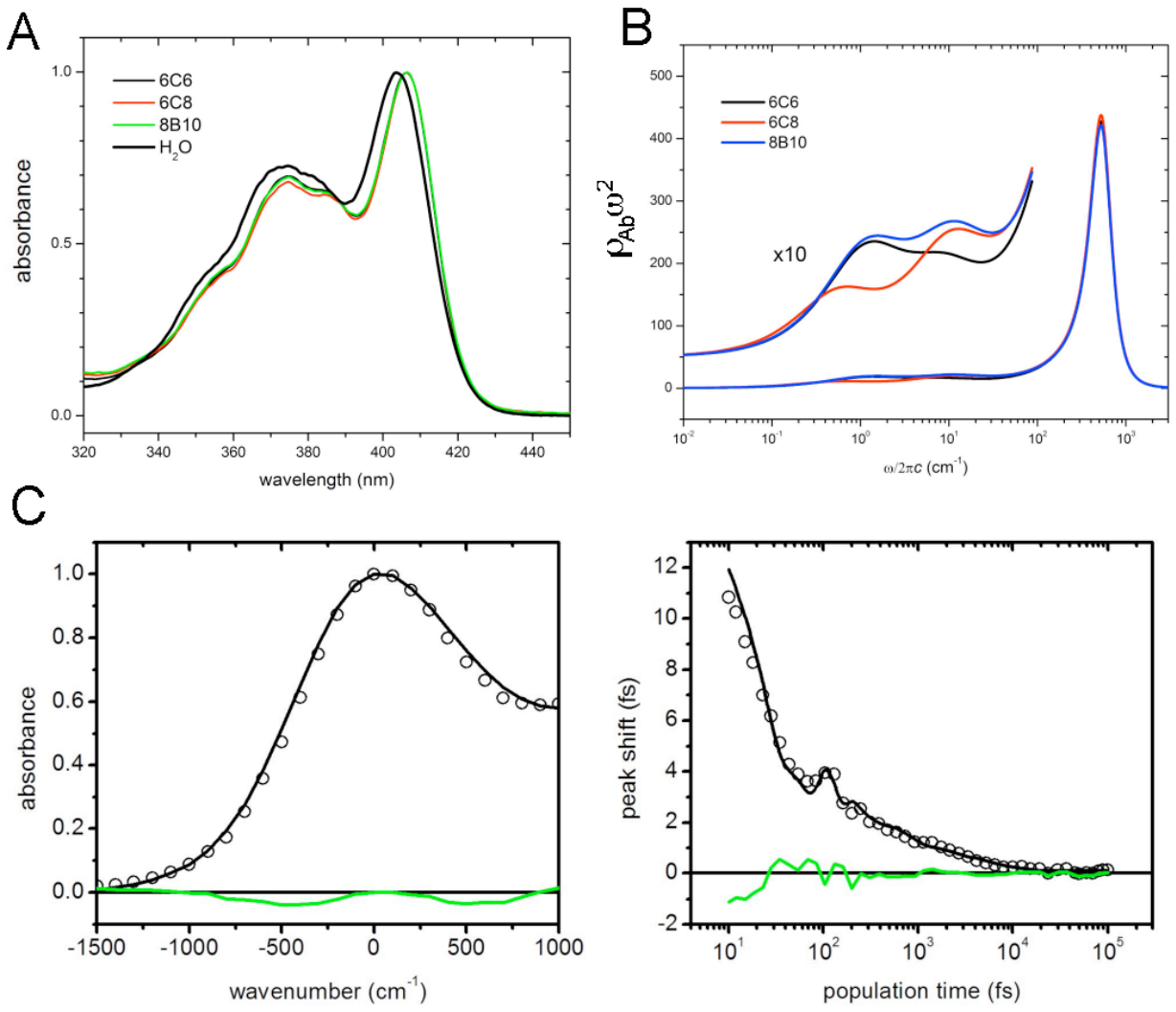

Figure S2. Steady-state absorption spectra, spectral densities, and a representative fit of absorption spectrum and 3PEPS decay. (A) Absorption spectra of MPTS/water and MPTS-Abs. (B) Spectral densities of Ab-MPTS complexes. (C) Absorption spectrum and 3PEPS decay of MPTS-8B10 complex (circles, data; black lines, best fit; green lines, residuals).

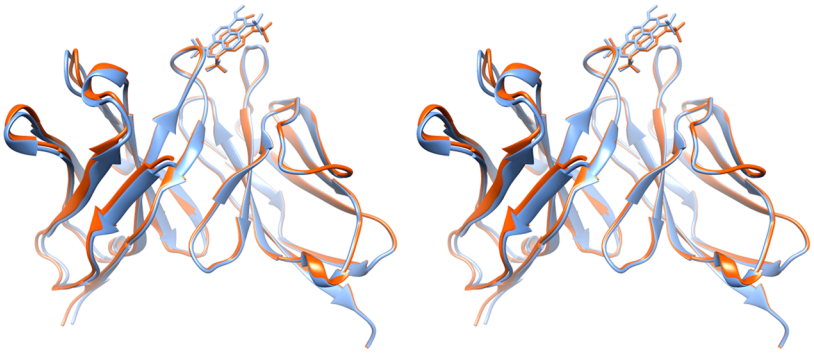

Figure S3. **Stereogram of a superposition of the constant regions of the 6c8 (blue) and 8b10 (red) MPTS complexes.** In both the 8B10 and 6C8 crystals, a symmetry-related Fab fragment packs against the face of the MPTS ligand. The two Fab-MPTS complexes crystallized in different space groups (see **Table 1**) and the packing contacts are different in the two structures. The 8B10 crystal packing contacts to MPTS (25 van der Waals contacts and 2 hydrogen bonds) come from neighboring light chain residues GlyL16, GlnL17 and IleL76, ProL77. In contrast, the 6C8 packing contacts to MPTS (32 van der Waals contacts and 2 hydrogen bonds) come from neighboring heavy chain residues TrpH199, ProH200, SerH202, and ProH227. Since the two structures are very similar despite the different packing interactions, we believe that that crystal packing is not affecting the conformation of the CDR loops or the binding mode of the ligand.

Nucleotide sequences of the V_L (variable light) and V_H (variable heavy) chains

>gl V_L
GACATTGTGCTGACCCAGTCTCCAGCTTCTTTGGCTGTGTCTCTAGGGCAGAGGGCCACCATATCCTGCAGAGCCAGTGAAAGTGTTGATA
GTTATGGCATTAGTTTTATGCACTGGTACCAGCAGAAACCAGGACAGCCACCCAAACTCCTCATCTATCGTGCATCCAACCTAGAATCTGG
GATCCCTGCCAGGTTCAGTGGCAGTGGGTCTAGGACAGACTTCACCCTCACCATTAATCCTGTGGAGGCTGATGATGTTGCAACCTATTAC
TGTCAGCAAAGTAATGAGGATCCTCGGACGTTCGGTGGAGGCACC

>gl V_H
GAGGTCCAGCTGCTCGAGTCTGGACCTGAGTTGGTGAAGCCTGGGGCTTCAGTGAAGATGTCCTGCAAGGCTTCTGGCTACACATTCACTG
ACTACTATATGCACTGGGTGAAGCAGAGCCATGGAAAGAGCCTTGAGTGGATTGGATATATTTATCCTAACAATGGTGGTAATGGCTACAA
CCAGAAGTTCAAGGGCAAGGCCACATTGACTGTAGACAAGTCCTCCAGCACAGCCTACATGGAGCTCCGCAGCCTGACATCTGATGACTCT
GCAGTCTATTACTGTGCAAGAAGAGGGGGCTACGGTATTAGAGGGTACTTCGATGTCTGGGGCGCAGGGACCACGGTCACC

>8B10 V_L
GACATTGTGCTGACCCAGTCTCCAGCTTCTTTGGCTGTGTCTCTAGGGCAGAGGGCCACCATATCCTGCAGAGCCAGTGAAAGTGTTGATA
GTTATGGCATTAGTTTTATGCACTGGTACCAGCAGAAACCAGGACAGCCACCCAAACTCCTCATCTATCGTGCATCCAACCTAGAATCTGG
GATCCCTGCCAGGTTCAGTGGCAGTGGGTCTAGGACAGACTTCACCCTCACCATTATTCCTGTGGAGGCTGATGATGTTGCAACCTATTAC
TGTCAGCAGAGTAATGAGGATCCTCGGACGTTCGGTGGAGGCACC

>8B10 V_H
GAGGTCCAGCTGCTCGAGTCTGGACCTGAGTTGGTGAAGCCTGGGACTTCAGTGAAGATGTCCTGCAAGGCTTCTGGCTACACATTCACTG
ACTACTACATGCACTGGGTGAAGCAGAGCCATGGCAAGAGCCTTGAGTGGATTGGATATATTTATCCTAACAATGGTGGTAATGGCTACAA
CCAGAAGTTCAAGGGCAAGGCCACATTGACTGTAGACAAGTCCTCCAGCACAGCCTACATGGAGCTCCGCAGCCTGACATCTGAAGACTCT
GCAGTCTATTACTGTGCAAGAAGAGGGGGCTACGGTAGTAGAGGATACTTCGATGTCTGGGGCGCAGGGACCACGGTCACC

>6C8 V_L
GACATTGTGCTGACCCAGTCTCCAGCTTCTTTGGCTGTGTCTTTAGGGCAGAGGGCCACCATATCCTGCAGAGCCAGTGAAAGTGTTGATA
GTTATGGCAATAGTTTTATGCACTGGTACCAGCAGAAACCAGGACAGCCACCCAAACTCCTCATCTATCGTGCATCCAACCTAGAATCTGG
GATCCCTGCCAGGTTCAGTGGCAGTGGGTCTAGGACAGACTTCACCCTCACCATTAATCCTGTGGAGGCTGATGATGTTGCAACCTATTAC
TGTCAGCAAAGTAATGAGGATCCTCGGACGTTCGGTGGAGGCACC

>6C8 V_H
GAGGTCCAGCTGCTCGAGTCTGGACCTGAGTTGGTGAAGCCTGGGGCTTCAGTGAAGATGTCCTGCAAGGCTTCTGGCTACACATTCACTG
ACTACTATATGCACTGGGTGAAGCAGAGCCATGGAAAGAGCCTTGAGTGGATTGGATATATTTATCCTAACAATGGTGGTAATGGCTACAA
CCAGAAGTTCAAAGGCAAGGCCACATTGACTGTAGACAAGTCCTCCAGCACAGCCTACATGGAGCTCCGCAGCCTGACATCTGATGACTCT
GCAGTCCATTACTGTGCAAGAAGAGGGGGCTACGGTATTAGAGGGTACTTCGATGTCTGGGGCGCAGGGACCACGGTCACC

>6C6 V_L
GACATTGTGCTGACCCAGTCTCCAGCTTCTTTGGCTGTGTCTCTAGGGCAGAGGGCCACCATATCCTGCAGAGCCAGTGAAAGTGTTAATA
GTTATGGCATTAGTTTTATGCACTGGTACCAGCAGAAACCAGGACAGCCACCCAAACTCCTCATCTATCGTGCATCCATCCTAGATTCTGG
GATCCCTGCCAGGTTCAGTGGCAGTGGGTCTAGGACAGACTTCACCCTCACCATTAATCCTGTGGAGGCTGATGATGTTGCAACCTATTAC
TGTCAGCAAAGTAATGAGGATCCTCGGACGTTCGGTGGAGGCACC

>6C6 V_H
GAGGTCCAGCTGCTCGAGTCTGGACCTGAGTTGGTGAAGCCTGGGGCTTCAGTGAAGATGTCCTGCAAGGCTTCTGGCTACACATTCACTG
ACTACTATATGCACTGGGTGAAGCAGAGCCATGGAAAGAGCCTTGAGTGGATTGGATATATTTATCCTAACAATGGTGATCATGGCTACAA
CCAGAAGTTCAAGGGCAAGGCCACATTGACTGTAGACAAGTCCTCCAGCACAGCCTACATGGAGCTCCGCAGCCTGACATCTGATGACTCT
GCAGTCTATTACTGTGCAAGAAGAGGGGGCTACGGTATTAGAGGGTACTTCGATGTCTGGGGCACAGGGACCACGGTCACC

Alignment of V_L nucleotide sequences

```
gl    VL   GACATTGTGCTGACCCAGTCTCCAGCTTCTTTGGCTGTGTCTCTAGGGCAGAGGGCCACC
8B10  VL   ------------------------------------------------------------
6C8   VL   ----------------------------------------T-------------------
6C6   VL   ------------------------------------------------------------

gl    VL   ATATCCTGCAGAGCCAGTGAAAGTGTTGATAGTTATGGCATTAGTTTTATGCACTGGTAC
8B10  VL   ------------------------------------------------------------
6C8   VL   ----------------------------------------A-------------------
6C6   VL   --------------------------A---------------------------------

gl    VL   CAGCAGAAACCAGGACAGCCACCCAAACTCCTCATCTATCGTGCATCCAACCTAGAATCT
8B10  VL   ------------------------------------------------------------
6C8   VL   ------------------------------------------------------------
6C6   VL   ------------------------------------------------T------T---

gl    VL   GGGATCCCTGCCAGGTTCAGTGGCAGTGGGTCTAGGACAGACTTCACCCTCACCATTAAT
8B10  VL   ------------------------------------------------------------T-
6C8   VL   ------------------------------------------------------------
6C6   VL   ------------------------------------------------------------

gl    VL   CCTGTGGAGGCTGATGATGTTGCAACCTATTACTGTCAGCAAAGTAATGAGGATCCTCGG
8B10  VL   ----------------------------------------G-------------------
6C8   VL   ------------------------------------------------------------
6C6   VL   ------------------------------------------------------------

gl    VL   ACGTTCGGTGGAGGCACC
8B10  VL   ------------------
6C8   VL   ------------------
6C6   VL   ------------------
```

Alignment of V_H nucleotides sequences

```
gl    VH   GAGGTCCAGCTGCTCGAGTCTGGACCTGAGTTGGTGAAGCCTGGGGCTTCAGTGAAGATG
8B10  VH   ----------------------------------------A-------------
6C8   VH   ------------------------------------------------------------
6C6   VH   ------------------------------------------------------------

gl    VH   TCCTGCAAGGCTTCTGGCTACACATTCACTGACTACTATATGCACTGGGTGAAGCAGAGC
8B10  VH   ------------------------------------C---------------------
6C8   VH   ------------------------------------------------------------
6C6   VH   ------------------------------------------------------------

gl    VH   CATGGAAAGAGCCTTGAGTGGATTGGATATATTTATCCTAACAATGGTGGTAATGGCTAC
8B10  VH   -----C------------------------------------------------------
6C8   VH   ------------------------------------------------------------
6C6   VH   ------------------------------------------------A-C---------

gl    VH   AACCAGAAGTTCAAGGGCAAGGCCACATTGACTGTAGACAAGTCCTCCAGCACAGCCTAC
8B10  VH   ------------------------------------------------------------
6C8   VH   --------------A---------------------------------------------
6C6   VH   ------------------------------------------------------------

gl    VH   ATGGAGCTCCGCAGCCTGACATCTGATGACTCTGCAGTCTATTACTGTGCAAGAAGAGGG
8B10  VH   -------------------------A----------------------------------
6C8   VH   ------------------------------------C---------------------
6C6   VH   ------------------------------------------------------------

gl    VH   GGCTACGGTATTAGAGGGTACTTCGATGTCTGGGGCGCAGGGACCACGGTCACC
8B10  VH   ----------G------A-------------------------------------
6C8   VH   ------------------------------------------------------
6C6   VH   ------------------------------------A-----------------
```

References

(1) Hornak, V., Abel, R., Okur, A., Strockbine, B., Roitberg, A., and Simmerling, C. (2006) Comparison of multiple Amber force fields and development of improved protein backbone parameters. *Proteins 65*, 712-725.

(2) Wang, J., Wolf, R. M., Caldwell, J. W., Kollman, P. A., and Case, D. A. (2004) Development and testing of a general amber force field. *J. Comput. Chem. 25*, 1157-1174.

(3) Jakalian, A., Bush, B. L., Jack, D. B., and Bayly, C. I. (2000) Fast, efficient generation of high-quality atomic charges. AM1-BCC model: I. Method. *Journal of computational chemistry 21*, 132-146.

(4) Walker, R. C., Crowley, M. F., and Case, D. A. (2008) The implementation of a fast and accurate QM/MM potential method in Amber. *J. Comput. Chem. 29*, 1019-1031.

(5) Case, D. A., Darden, T. A., Cheatham, T. E. I., Simmerling, C. L., Wang, R. E., Duke, R. E., Luo, R., Walker, R. C., Zhang, W., Merz, K. M., Roberts, B., Hayik, S., Roitberg, A., Seabra, G., Swails, J., Götz, A. W., Kolossváry, I., Wong, K. F., Paesani, F., Vanicek, J., Wolf, R. M., Liu, J., Wu, X., Brozell, S. R., Steinbrecher, T., Gohlke, H., Cai, Q., Ye, X., Wang, J., Hseih, M.-J., Cui, G., Roe, D. R., Mathews, D. H., Seetin, M. G., Salomon-Ferrer, R., Sagui, C., Babin, V., Luchko, T., Gusarov, S., Kovalenko, A., and Kollman, P. A. (2012), AMBER 12, University of California, San Francisco.

(6) Salomon-Ferrer, R., Case, D. A., and Walker, R. C. (2013) An overview of the Amber biomolecular simulation package. *WIREs Comput. Mol. Sci. 3*, 198-210.

(7) Jorgensen, W. L., Chandrasekhar, J., Madura, J. D., Impey, R. W., and Klein, M. L. (1983) Comparison of simple potential functions for simulating liquid water. *J. Chem. Phys. 79*, 926-935.

(8) Grand, S. L., Götz, A. W., and Walker, R. C. (2013) SPFP: Speed without compromise—A mixed precision model for GPU accelerated molecular dynamics simulations. *Computer Physics Communications 184*, 374-380.

(9) Salomon-Ferrer, R., Götz, A. W., Poole, D., Le Grand, S., and Walker, R. C. (2013) Routine microsecond molecular dynamics simulations with AMBER on GPUs. 2. Explicit solvent particle mesh ewald. *J. Chem. Theory Comput. 9*, 3878-3888.

(10) Roe, D. R., and Cheatham, T. E. (2013) PTRAJ and CPPTRAJ: Software for Processing and Analysis of Molecular Dynamics Trajectory Data. *J. Chem. Theory Comput. 9*, 3084-3095.

(11) Mukamel, S. (1995) *Principles of Nonlinear Optical Spectroscopy*, Oxford University Press, New York.

(12) Jimenez, R., Case, D. A., and Romesberg, F. E. (2002) Flexibility of an antibody binding site measured with photon echo spectroscopy. *J. Phys. Chem. B 106*, 1090-1103.

(13) Cho, M., Yu, J.-Y., Joo, T., Nagasawa, Y., Passino, S. A., and Fleming, G. R. (1996) The integrated photon echo and solvation dynamics. *J. Phys. Chem. 100*, 11944-11953.

(14) de Boeij, W. P., Pshenichnikov, M. S., and Wiersma, D. A. (1996) System-bath correlation function probed by conventional and time-grated stimulated photon echo. *J. Phys. Chem. 100*, 11806-11823.